Available online at www.sciencedirect.com
ScienceDirect
Journal of the European Ceramic Society 30 (2010) 107–112
www.elsevier.com/locate/jeurceramsoc

The effect of SiO_2 addition on the development of low-Σ grain boundaries in PTC thermistors

M.A. Zubair, C. Leach *

Materials Science Centre, School of Materials, University of Manchester, Manchester, M1 7HS, UK

Received 30 January 2009; received in revised form 7 July 2009; accepted 22 July 2009
Available online 4 September 2009

Abstract

Electron backscatter pattern analysis has been used to characterise, using the coincidence site lattice model, the distribution of grain boundary structures in a series of $BaTiO_3$ based positive temperature coefficient of resistance (PTC) thermistors, prepared with 0, 1.0, 2.0 and 3.0 at.% SiO_2 additions. As the SiO_2 content was raised, the proportion of random, high-angle grain boundaries in the microstructure increased steadily from 85.7% to 89.6%, while the proportion of grain boundaries indexable in the range Σ3–Σ29 decreased from 14.3% to 10.4%, and the Σ3 grain boundary population fell from 5.9% to 3.6%. At the same time the proportion of Σ3 twin boundaries remained approximately constant at 3.0 ± 0.3%. Significantly more Σ3 grain boundaries than would be expected in a randomly oriented, untextured material were observed in all samples. The variation in grain boundary types with SiO_2 addition is discussed in terms of grain boundary energy and its effect on PTC performance.

Keywords: Electroceramic; Positive temperature coefficient (PTC); Electron backscattering patterns (EBSP); Grain boundary structure; Coincidence lattice

1. Introduction

Positive temperature coefficient of resistance (PTC) thermistors, based on sintered, polycrystalline donor and acceptor co-doped $BaTiO_3$ ceramics show a significant increase in grain boundary resistivity at temperatures just above the ferro- to para-electric transition temperature, T_C. This PTC effect is attributed to the appearance of a back-to-back Schottky-type grain boundary potential barrier just above T_C, and arises from the combined effects of the disappearance of spontaneous polarisation, the temperature dependency of dielectric constant and the presence of filled acceptor traps at the grain boundaries [1–4].

It has been reported widely that the magnitude and temperature profile of the resistance jump associated with the PTC transition can differ significantly between individual grain boundaries [5–9]. These variations have previously been attributed to microchemical inhomogeneities [10,11] or to differences in interface geometry, the latter often being described in terms of the coincidence-site lattice (CSL) model [12]. Using CSL terminology it has been reported that Σ3, Σ5 and Σ9 grain boundaries characteristically tend to show little or no PTC effect [13–16], whereas random, high-angle grain boundaries generally exhibit large resistance jumps in the PTC region. These differences in behaviour with grain boundary type have been attributed to changes in the magnitude of the oxygen diffusion coefficient, which affects the rate of grain boundary reoxidation during the cooling stage of the sintering cycle and hence the density of occupied interface states in the final microstructure [15].

A previous study of a sintered $BaTiO_3$ found that 9.0% of all interfaces could be indexed as Σ3, a value greatly in excess of the 2.7% calculated to occur by chance in a microstructure composed of randomly oriented grains [17], while a subsequent study of a commercial PTC thermistor, with 2.0% SiO_2 addition, reported that 4.7% of all grain boundaries were found to have a Σ3 misorientation [18]. In the latter study it was also noted that this population of Σ3 grain boundaries formed at an early stage of sintering and was retained in the microstructure during grain growth. The observation that such grain boundary types, which are reported to be PTC inactive [13,14], can form preferentially during sintering is important in attempts to optimise the performance of PTC thermistors, since microstructures containing a significant proportion of grain boundaries where the PTC effect is weak, or absent, are undesirable.

* Corresponding author.
E-mail address: colin.leach@manchester.ac.uk (C. Leach).

0955-2219/$ – see front matter © 2009 Elsevier Ltd. All rights reserved.
doi:10.1016/j.jeurceramsoc.2009.07.026

SiO_2 has long been added to $BaTiO_3$ as a sintering and performance aid, lowering the sintering temperature by promoting liquid-phase sintering, reducing the grain size distribution and allowing the formation of semiconducting grains at lower temperatures [19]. It has also been reported that the addition of SiO_2 decreases the resistivity of the thermistor below T_C, and reduces the magnitude of the resistivity jump, while displacing the temperature of peak resistivity to higher temperatures, which also has the effect of reducing the gradient of the characteristic PTC resistance-temperature curve in the PTC region [20].

In this contribution electron backscatter pattern (EBSP) analysis has been used to investigate the role of SiO_2 addition on microstructural development in PTC thermistors, particularly with regard to grain boundary structure and morphology.

2. Method

Four thermistor samples, containing 0, 1.0, 2.0 and 3.0 at.% SiO_2 additions, were prepared by a mixed oxide route from $(Ba,Ca)TiO_3$, co-doped with a rare earth donor and 0.1% Mn acceptor ions. Powder compacts were pressed and sintered in air at a temperature of 1300 °C for 1 h and cooled at 5 °C min^{-1}, producing fully sintered, dense pellets 8 mm in diameter and 2 mm in thickness. Cross-sections of the pellets were prepared for microstructural analysis by grinding, diamond polishing, and finishing with a colloidal silica solution to produce a near strain-free surface finish.

Microstructural characterisation was carried out using backscattered electron (BS) imaging and EBSP analysis, in a Phillips XL30 FEGSEM equipped with an HKL EBSP system and software [21]. The step size during analysis was 0.2 μm, allowing several data points to be collected from within each grain. An in-house program [22] was used to establish the relative abundances of low Σ interfaces, from Σ3 to Σ29 inclusive, that were present in the thermistor. All grain boundaries not indexable in this way were classified as random, high-angle. High resolution microscopy of grain boundary structures was carried out using a TECNAI F30 300 keV transmission electron microscope (TEM).

3. Results

Resistance-temperature graphs for these thermistors have been presented previously [20]. Fig. 1(a–d) shows BS images of the PTC thermistors with SiO_2 additions of 0, 1.0, 2.0 and 3.0 at.% respectively. Twinning is observed in all samples. The major twins bisecting the grains have a Σ3 misorientation, but were considered separately from the grain boundaries for the purpose of establishing interface population statistics. The mean grain size was measured using the linear intercept technique and lay in the range 6.3 ± 0.5 μm for all samples, indicating that SiO_2 additions of up to 3.0 at.% do not have a significant effect on overall grain growth. However, increasing the SiO_2 content did reduce the grain size distribution markedly and cause the predominant grain shape to change from rounded to square, due to the development of a {1 0 0} habit. The change in grain shape suggests that in $BaTiO_3$ the energies of crystallographically distinct grain faces are modified by the addition of SiO_2, with the overall consequence that the relative surface energy and

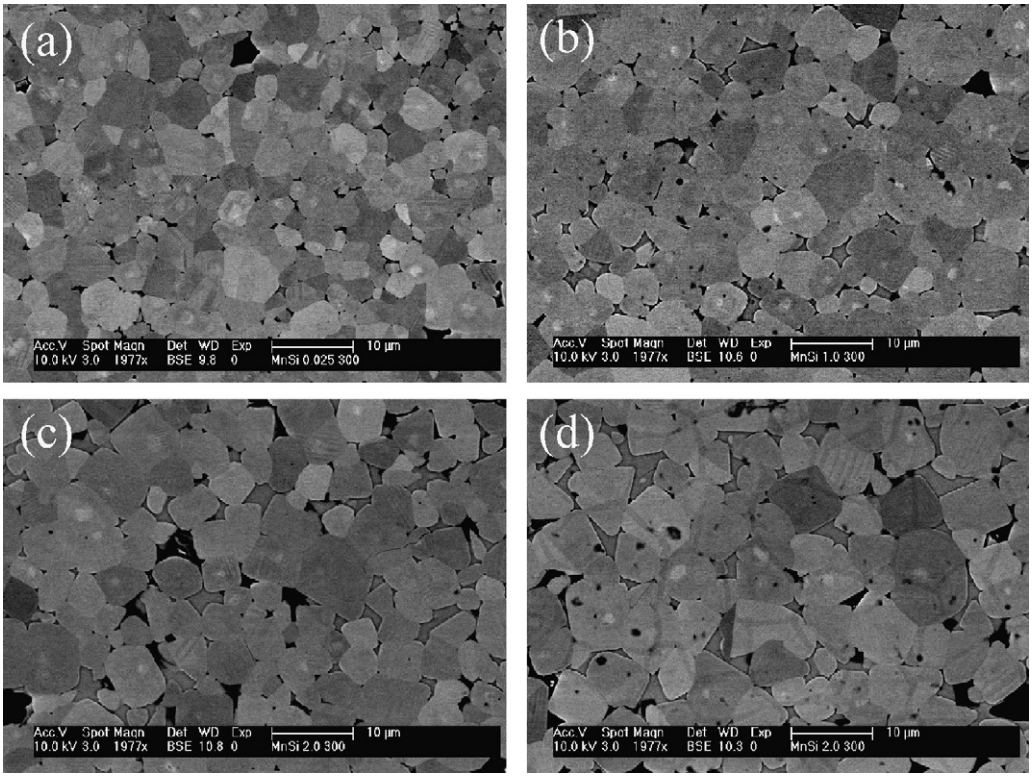

Fig. 1. Backscattered electron images of samples with (a) 0 at.% SiO_2 (b) 1.0 at.% SiO_2 (c) 2.0 at.% SiO_2 (d) 3.0 at.% SiO_2. Scale bar = 10 μm.

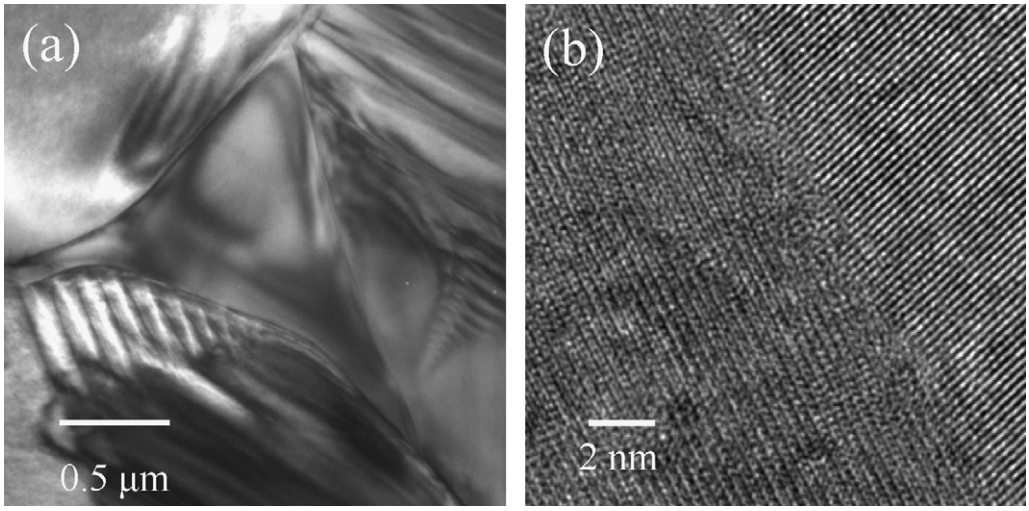

Fig. 2. TEM images of (a) triple junction containing second phase (scale bar = 0.5 μm), and (b) high resolution image of 'clean' grain boundary (scale bar = 2 nm).

growth rate of the {1 0 0} planes is reduced as the SiO_2 content is increased, eventually causing the {1 0 0} habit to dominate the microstructure.

XRD identified the second phase, present in all samples with SiO_2 addition, as fresnoite. Its distribution was limited to triple junctions (Fig. 2a), with no evidence, even in high resolution TEM images, for an intergranular film that would suggest grain boundary wetting (Fig. 2b). Cheng [23] also noted an absence of grain boundary film in his study of the effect of SiO_2 and TiO_2 additions in this system. In order to explain the microstructural changes he observed, it was proposed that SiO_2 or TiO_2 addition led to the formation of a wetting silicate phase at PTC thermistor grain boundaries during sintering, but that this film withdrew on cooling, and collected at triple junctions. Choi et al. [24] observed intergranular films of varying thickness in TiO_2-rich $BaTiO_3$ and attributed their development to the progressive penetration of a liquid-phase, which initially accumulated at triple junctions, along the grain boundaries. Our observation of grain size homogenisation and changes in grain morphology with SiO_2 addition are also most simply explained in terms of a percolating, second phase film, which was present at the grain boundaries during sintering, and which became more prevalent with increasing SiO_2 addition. This film modified the surface and interfacial energies of the $BaTiO_3$ grains, causing them to grow with differing morphologies, possibly as a consequence of the change in surface Ba:Ti ratio as fresnoite formed, but subsequently withdrew to triple junctions on cooling, to give the final distribution in the microstructure, in line with our observations and the proposals of other workers [23,24].

The distribution of grain boundary types and twin structures present in each sample were characterised using EBSP analysis. An area close to the centre of each pellet, approximately 250 μm × 200 μm in size, was selected for analysis, allowing around 3000 interfaces to be characterised in each case (Table 1). The interfaces were classified, where possible, using CSL nomenclature for Σ values up to Σ29: any remaining boundaries that could not be indexed in this way were classified as random, high-angle. Fig. 3(a–d) are ⟨1 0 0⟩ pole figures showing the distribution of grain orientations in each sample. The uniformity of the distributions indicates that there is no significant preferred grain orientation and hence no crystallographic texture that might influence the distribution of grain boundary types found within the thermistors. Table 1 summarises the grain boundary misorientation data by listing the proportions of high-angle grain boundaries and low-Σ grain boundaries in each sample as a function of the total grain boundary population. The abundances of Σ3 twin boundaries within each microstructure, as a function of the total interface population, are also included. Several trends are apparent. On increasing the SiO_2 content from 0% to 3.0 at.% the proportion of random high-angle grain boundaries increases progressively from 85.7% to 89.6%, reducing the population of grain boundaries indexable in the range Σ3–Σ29 from 14.3% to 10.4%. Within this group the Σ3 grain boundary population shows the most significant change, decreasing from 5.9% to 3.6%. Given the sample size, both of these variations are statistically significant and systematic with SiO_2 addition. The distribution and variation with SiO_2 addition of all Σ indexable grain boundaries are summarised in

Table 1
Grain boundary and twin population statistics as a function of SiO_2 addition.

SiO_2 content (at.%)	Total grain boundaries analysed	% high-angle grain boundaries	% Σ3–Σ29 grain boundaries	% Σ3 grain boundaries	% Σ5–Σ29 grain boundaries	% Σ3 twin boundaries
0.0	2867	85.7	14.3	5.9	8.4	2.8
1.0	3691	86.0	14.0	5.1	8.9	2.7
2.0	3447	87.6	12.4	4.3	8.1	3.3
3.0	3635	89.6	10.4	3.6	6.8	3.3

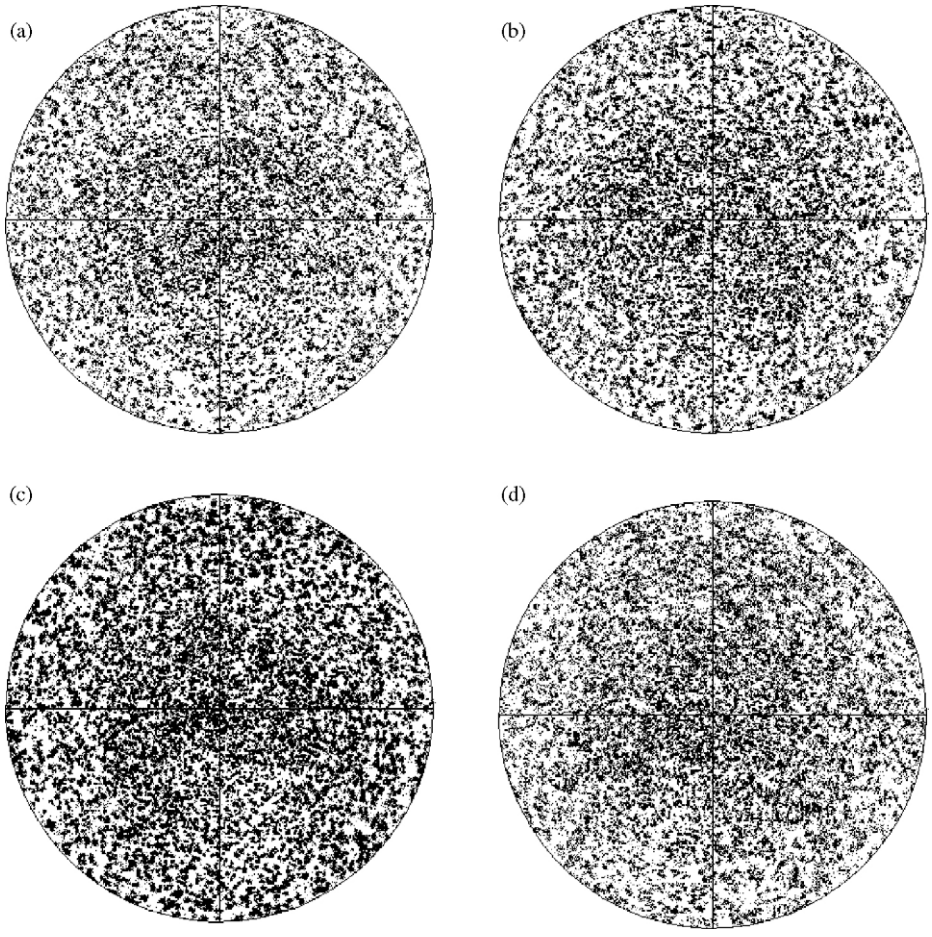

Fig. 3. {1 0 0} polefigures showing grain orientation distributions in samples sintered with SiO_2 additions of (a) 0 at.%, (b) 1.0 at.%, (c) 2.0 at.%, and (d) 3.0 at.%.

Fig. 4, from which it can be seen that other low-Σ grain boundary structures, notably Σ5, Σ9 and Σ11, also show a small reduction in abundance with increasing SiO_2 content. However in most other cases any variation is difficult to confirm due to statistical noise associated with the small numbers involved, although when grain boundaries in the range Σ5–Σ29 are considered together, there is an overall decrease in the total population from 8.4% to 6.8%. Despite this progressive reduction in the proportion of low-Σ grain boundaries with SiO_2 addition, the Σ3 twin population remained relatively constant throughout, lying in the range $3.0 \pm 0.3\%$, which is consistent with a previous study that noted the twin density is controlled by mean grain size, and reflects a relaxation of accumulated stress [18].

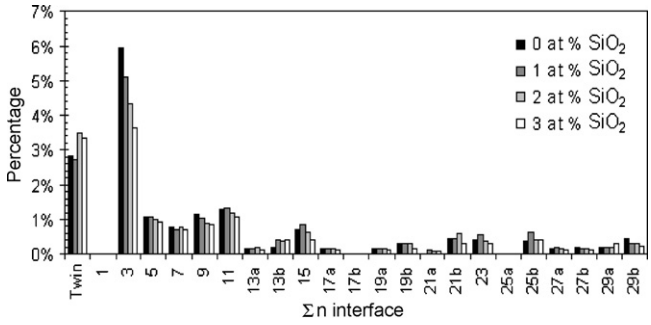

Fig. 4. Histogram showing variation of low-Σ grain boundary abundance by Σ value, as a function of SiO_2 addition.

In all of the samples studied here there are significantly more Σ3 grain boundaries than would be expected to occur by chance within a random distribution of grain orientations (around 2.7%): an observation that is in agreement with the findings of earlier workers [17,18]. We also note that with SiO_2 addition there are progressive decreases, both in the proportion of Σ3 grain boundaries, and in the total number of grain boundaries indexable in the range Σ5–Σ29. The tendency to form and retain a high proportion of Σ indexable grain boundaries in the sintered microstructure is therefore strongest in the samples where there is little or no SiO_2 addition. We believe that the proportion of Σ grain boundaries decreases as the SiO_2 content is increased because the presence of SiO_2 changes the relative energies of differently structured grain boundaries during sintering with the consequence that their relative abundances in the microstructure change. Previous workers have shown using a statistical approach, that in many microstructures, certain crystal faces occur preferentially at grain boundaries with specific misorientations and hence that grain boundaries preferentially adopt certain structures in sintered materials [25–27]. The particular structures that are favoured depend on the system: for example $SrTiO_3$

shows a strong tendency to form ⟨1 0 0⟩ type grain boundary planes at 15° grain misorientation [25], in MgO [1 0 0] planes occur preferentially at all misorientations [26], and in alpha-brass asymmetric ⟨1 1 0⟩ tilt boundaries and ⟨1 1 1⟩ twist boundaries were found to predominate [27]. The driving force is an overall energy reduction through the preferential formation and retention of low energy grain boundary structures, and has been validated by the derivation of an approximately inverse relationship between the energy of a particular grain boundary structure and its frequency of occurrence in the microstructure [28].

CSL Σ boundaries are defined using geometrical criteria [12] that indicate grain boundary misorientations where a simple interfacial atomic configuration might occur, reducing the energy of the grain boundary. In $BaTiO_3$ this is believed to be the case for Σ3 grain boundaries, which occur preferentially in the microstructure, and which are commonly described as coherent, low energy structures with low defect concentrations and little or no impurity segregation [29]. These latter characteristics are consistent with the weak PTC behaviour associated with these grain boundary types [13,14,29] and are indicative of limited wetting and dopant transport along these grain boundaries during sintering, reducing trap formation and activation. The weak PTC effect, similarly reported for Σ5 and Σ9 grain boundaries [12] also suggests that these grain boundaries also adopt low energy structural configurations with a reduced driving force for dopant segregation at the interface. The energies of 'randomly oriented' high-angle grain boundaries, however, are generally accepted to be higher than 'special', low-Σ grain boundaries due to increased lattice mismatch and associated interfacial disorder [30]. Consequently there is the possibility that the energy of a high-angle grain boundary may be lowered significantly by the incorporation of appropriate segregants that can accommodate lattice strain, or a low melting-point sintering aid that wets the interface [29].

As the SiO_2 content is increased, the volume of liquid phase formed at the sintering temperature will increase. If it is the case, as has previously been suggested [23], that the liquid does not remain confined to triple junctions at the peak sintering temperature, then there must either be an increase in grain boundary coverage by the film, or an overall increase in its thickness [23,24]. A recent study of grain boundary structures in doped Al_2O_3 demonstrated that a series of interfacial phases with differing structures can form and co-exist in the same sample with their energies, and hence populations, governed by factors such as grain boundary type, additive levels, and sintering temperature [31]. Each structure was associated with a grain boundary of different mobility, a property which is also dependent on interfacial energy, demonstrating that film structure and overall grain boundary energy are closely related. In our case the interfacial energy of high-angle grain boundaries is also likely to be interlinked with the progressive, concomitant change in crystal habit towards {1 0 0} with increasing SiO_2.

Thus in $BaTiO_3$ a mechanism exists to reduce progressively the overall energy difference between the high-angle and certain low-Σ grain boundaries during sintering through the incorporation of an increasing volume of a wetting phase, which contains dissolved grain boundary segregants, and which only effectively percolates the higher energy, high-angle grain boundaries. This has the consequence that, with increasing SiO_2, the energy advantage associated with the formation of a high proportion of low-energy, low-Σ grain boundaries, and Σ3 grain boundaries in particular but possibly also Σ5, Σ9 and Σ11, is reduced leading to a lower population of such interfaces in the ceramic, as we observe. The progressive increase in the proportion of random, high-angle grain boundaries and the increasing development of {1 0 0} habit with SiO_2 addition further indicates that this reduction in grain boundary energy associated with the high-angle grain boundaries, when compared with certain low-Σ grain boundaries, occurs cumulatively with increasing SiO_2.

Since Σ3, Σ5 and Σ9 interfaces have all been reported as being PTC inactive, or at least to show a significantly reduced PTC effect [14,15], a high proportion of such grain boundaries in PTC thermistors will have a significant effect in modifying the overall device performance, especially with regard to the overall magnitude of the PTC jump and the homogeneity of current flow during high power switching transients. The combined total of Σ3, Σ5 and Σ9 interfaces in our samples reduced from 8.1% to 5.4% on increasing the SiO_2 level from 0 to 3 at.%, the majority of this change coming from the reduction in the proportion of Σ3 grain boundaries, although downward trends were also observed in the Σ5 and Σ9 grain boundary populations. Thus although there still remains the possibility of a significant number of poorly performing PTC thermistor grain boundaries being present in the microstructure, their overall population can be reduced by a third with 3.0 at.% SiO_2 addition.

4. Conclusions

A series of $BaTiO_3$ based PTC thermistors was prepared with SiO_2 additions in the range 0–3.0 at.%, and the proportions of grain boundaries corresponding to certain CSL types were characterised. The samples were untextured, but all contained significantly more Σ3 grain boundaries than would be expected by chance. The proportion of Σ3 grain boundaries decreased significantly with increasing SiO_2 addition, as did the overall population of other grain boundaries in the range Σ5–Σ29, with Σ5, Σ9 and Σ11 grain boundaries independently showing small reductions with increasing SiO_2. Simultaneously the proportion of high-angle grain boundaries increased, while the abundance of Σ3 twin boundaries in the microstructure remained approximately constant. The change in the proportions of grain boundary structural types with SiO_2 addition was explained in terms of preferential wetting of random, high-angle grain boundaries by a SiO_2 rich film at the sintering temperature, which reduces their energy, whilst having little effect on the energies of other low-energy low-Σ boundaries.

Acknowledgments

Financial support from the University of Manchester, ORS and GE Sensing is acknowledged.

References

1. Heywang, W., Resistivity anomaly in doped barium titanate. *J. Am. Ceram. Soc.*, 1964, **47**, 484–490.
2. Goodman, G., Electrical conduction anomaly in samarium doped barium titanate. *J. Am. Ceram. Soc.*, 1963, **46**, 48–54.
3. Jonker, G. H., Some aspects of semiconducting barium titanate. *Solid State Electron.*, 1964, **7**, 895–903.
4. Jonker, G. H., Equilibrium barriers in PTC thermistors. In *Adv. In Ceramics 1, Grain Boundary Phenomena in Electronic Ceramics*, ed. L. M. Levinson. Am. Ceram. Soc., 1981, pp. 155–166.
5. Gerthsen, P. and Hofmann, B., Current-voltage characteristics and capacitance of single grain boundaries in semiconducting $BaTiO_3$ ceramics. *Solid State Electron.*, 1973, **16**, 617–622.
6. Nemoto, H. and Oda, I., Direct examinations of PTC action of single grain. *J. Am. Ceram. Soc.*, 1980, **63**, 398–401.
7. Kuwabara, M., Morimo, K. and Matsunaga, T., Single-grain boundaries in PTC resistors. *J. Am. Ceram. Soc.*, 1996, **79**, 997–1001.
8. Leach, C., Russell, J. D. and Wood, G. I., Direct observation of resistive barriers in a $BaTiO_3$ based thermistor. *J. Mater. Sci.*, 1997, **32**, 4641–4643.
9. Russell, J. D., Leach, C. and Freer, R., Grain boundary structures in electronic ceramics. *Key Eng. Mater.*, 1997, **132–136**, 1155–1158.
10. Desu, S. B. and Payne, D. A., Interfacial segregation in Perovskites: IV, Internal boundary layer devices. *J. Am. Ceram. Soc.*, 1990, **73**, 3416–3421.
11. Blamey, J. M. and Parry, T. V., The effect of processing variables on the mechanical and electrical properties of barium titanate PTCR ceramics (Part 1). *J. Mater. Sci.*, 1993, **28**, 4311–4316.
12. Randle, V., *The Measurement Of Grain Boundary Geometry*. IOP publishing, Bristol, UK, 1993.
13. Ogawa, H., Demua, M., Yamamoto, T. and Sakuma, T., Estimation of the PTCR effect in single grain boundary of Nb-doped $BaTiO_3$. *J. Mater. Sci.*, 1995, **14**, 537–538 (letters).
14. Hayashi, K., Yamamoto, T. and Sakuma, T., Grain orientation dependence of the PTCR effect in niobium-doped barium titanate. *J. Am. Ceram. Soc.*, 1996, **79**, 1669–1672.
15. Hayashi, K., Yamamoto, T., Ikuhara, Y. and Sakuma, T., Grain boundary electrical barriers in PTC thermistors. *J. Appl. Phys.*, 1999, **86**, 2909–2913.
16. Hayashi, K., Yamamoto, T., Ikuhara, Y. and Sakuma, T., Formation of potential barrier related to grain boundary character in semiconducting barium titanate. *J. Am. Ceram. Soc.*, 2000, **83**, 2684–2688.
17. Ernst, F., Mulvihill, M. L., Kienzle, O. and Ruhle, M., Preferred grain orientation relationships in sintered perovskite ceramics. *J. Am. Ceram. Soc.*, 2001, **84**, 1885–1890.
18. Seaton, J. and Leach, C., Formation and retention of low-Σ interfaces in PTC thermistors. *Acta Mater.*, 2005, **53**, 2751–2758.
19. Roseman, R. D. and Mukherjee, N., PTCR Effect in $BaTiO_3$: structural aspects and grain boundary potentials. *J. Electroceram.*, 2003, **10**, 117–135.
20. Zubair, M. A. and Leach, C., Modeling the effect of SiO_2 additions and cooling rate on the electrical behavior of donor–acceptor co-doped positive temperature coefficient thermistors. *J. Appl. Phys.*, 2008, **103**, article 123713.
21. Channel 5 diffraction pattern analysis software, HKL, Denmark.
22. Humphreys, F. J., *Vmap 8.5, School of Materials*. University of Manchester, Manchester, UK, 2001.
23. Cheng, H., Effect of sintering aids on the electrical properties of positive temperature coefficient of resistivity $BaTiO_3$ ceramics. *J. Appl. Phys.*, 1989, **66**, 1382–1387.
24. Choi, S. Y., Yoon, D. Y. and Kang, S. J. L., Kinetic formation and thickening of intergranular amorphous films at grain boundaries in barium titanate. *Acta Mater.*, 2004, **52**, 3721–3726.
25. Saylor, D. M., El-Dasher, B. S., Adams, B. L. and Rohrer, G. S., Measuring the five-parameter grain boundary distribution from observations of planar sections. *Metall. Mater. Trans. A: Phys. Metall. Mater. Sci.*, 2004, **35A**, 1981–1989.
26. Saylor, D. M., Moraweic, A. and Rohrer, G. S., The relative free energies of grain boundaries as a function of five macroscopic parameters. *Acta Mater.*, 2003, **51**, 3675–3686.
27. Kim, C. S., Hu, Y., Rohrer, G. S. and Randle, V., Five-parameter grain boundary distribution in grain boundary engineered brass. *Scripta Mater.*, 2005, **52**, 633–637.
28. Saylor, D. M., Moraweic, A. and Rohrer, G. S., Distribution and energies of grain boundaries in magnesia as a function of five degrees of freedom. *J Am. Ceram. Soc.*, 2002, **85**, 3081–3083.
29. Krasevec, V., Drofenik, M. and Kolar, D., Genesis of the (1 1 1) twin in barium titanate. *J. Am. Ceram. Soc.*, 1990, **73**, 856–860.
30. Clarke, D. R., Intergranular phases in polycrystalline ceramics. In *Surfaces an Interfaces of Ceramic Materials, NATO ASI series*, *vol 173*, ed. Dufour, Monty and Petot-Ervas. Kluwer academic publishers, 1988, pp. 57–79.
31. Dillon, S. J. and Harmer, M. P., Demystifying the role of sintering additives with 'complexation'. *J. Eur. Ceram. Soc.*, 2008, **28**, 1485–1493.